

Origin of the C-induced $p4g$ reconstruction of Ni(001)

Sergey Stolbov, Sampyo Hong, Abdelkader Kara, and Talat S. Rahman

Department of Physics, Kansas State University, 116 Cardwell Hall, Manhattan, Kansas 66506, USA

(Received 19 April 2005; revised manuscript received 29 August 2005; published 19 October 2005)

First principles calculations of the geometric and electronic structures have been performed for two coverages (0.25 ML and 0.5 ML) of C on Ni(001) to understand the mechanism of the Ni(001) reconstruction induced by carbon adsorption. The calculated structural behavior of the system is in a good agreement with experimental observations. The calculated path and energetics of the $c(2\times 2)-p4g$ reconstruction in $C_{0.5}/\text{Ni}(001)$ is provided. A dramatic reduction of the local electronic charge on adsorbed carbon is found to occur upon the reconstruction that decreases the electron-electron repulsion on C site. This effect together with the formation of covalent bonds between C and the second layer Ni atoms, leads to reconstruction of Ni(001).

DOI: [10.1103/PhysRevB.72.155423](https://doi.org/10.1103/PhysRevB.72.155423)

PACS number(s): 68.43.Fg

I. INTRODUCTION

Nickel is used as a catalyst for many reactions. The presence of carbon in the reaction environment may lead to atomic adsorption on the metal surface changing the electronic structure and consequently its reactivity.¹ It is thus important to understand the mechanism by which C adsorbs on Ni surfaces. On the other hand, this system is an excellent prototype for addressing fundamental issues such as the effects of the adsorption of light elements on the electronic and geometric structures of metal substrate and the character of the chemical bonding between the adsorbate and the surface. It is thus not surprising that the first observation of C induced reconstruction of Ni(001)² has attracted the attention of experimentalists and theorists who aim to provide an increasingly accurate description and explanation of the nature of this phenomenon.²⁻¹⁴

It is well-known that when carbon adsorbs on Ni(001) with coverage less than one third of a monolayer (ML) it occupies hollow sites and does not change the symmetry of the outmost metal layers.³ As the coverage exceeds 0.33 ML, the surface reconstructs to what has become known as “the clock reconstruction”.²⁻⁴ Figure 1 illustrates schematically these two geometries, in which both C atoms occupy the fourfold hollow sites. In the reconstructed structure, the topmost Ni atoms (Ni1) are displaced parallel to the surface by alternate clockwise and counterclockwise rotations around C, forming a geometry of the $(2\times 2)p4g$ symmetry. A large volume of additional information has also been obtained from more recent experiments. Scanning tunnel microscope (STM)³ and photoelectron diffraction (PhD)⁴ measurements have been performed for nonreconstructed Ni(001) with the C coverage less than 0.3 ML ($C_\theta/\text{Ni}(001)$, $\theta < 0.3$ ML). Although the quantitative results in the two papers differ, both report a small outward radial displacement of the Ni1 atoms around the C adsorbate. On the other hand, low energy electron diffraction (LEED)⁵ and PhD⁴ experiments, performed for larger coverage ($\theta > 0.33$ ML), revealed the main sign of the reconstruction, rotations of Ni1 atoms around C. The magnitude of Ni1 displacements (Δ_{xy}) caused by these rotations is found to be 0.4-0.55 Å. The authors also observed a penetration of C atoms into the Ni1 layer accompanying the reconstruction.

The nature of this reconstruction has been the subject of much debate in the past two decades. Using a simple force constant model in lattice dynamical calculations, Rahman *et al.*^{6,7} have suggested that the reconstruction is driven by

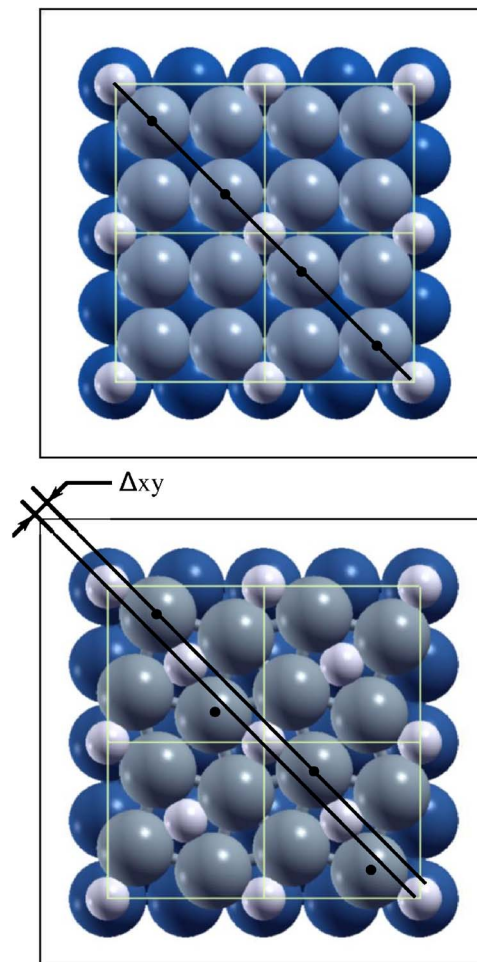


FIG. 1. (Color online) An illustration of the $p(2\times 2)C_{0.25}/\text{Ni}(001)$ (upper panel) and $p4gC_{0.5}/\text{Ni}(001)$ (lower panel) geometric structures. Black dots mark the centers of some Ni1 atoms. Δ_{xy} characterizes displacement of Ni1 atoms caused by their rotation about C during the reconstruction.

phonon softening. Several scenarios for the reduction of specific force constants were presented, including those involving the coupling of C to the Ni atoms in the second layer (Ni2)^{2,3,7,10} which seems plausible since C penetrates the surface during the reconstruction. On the other hand, Terborg *et al.*⁴ argued that the reconstruction is caused by C-induced Ni1-Ni1 repulsion rather than by C-Ni2 bonding, a conclusion that is supported by recent band structure calculations.¹⁴ Charge transfer between C and N atoms has also been suggested to be a factor controlling the reconstruction.^{8,9} However, to our knowledge, the distribution of local charges in the C/Ni(001) system has not yet been calculated from first principles. It has also been proposed that surface stress^{10,11} might be responsible for the reconstruction. First principles calculations of C induced surface stress on Ni(001), however, do not reveal any specific relationship between surface stress and surface reconstruction.¹³ *Ab initio* calculations by Alfe *et al.*¹² also emphasize the importance of chemical bonding rather than elastic effects for the reconstruction. Both of these sets of *ab initio* calculations, based on density functional theory in the plane wave pseudopotential (PWPP) representation and with the local density approximation for the exchange-correlation potential, have also addressed the issue of geometric and electronic structural changes brought about by the adsorption of 0.5 ML of C on Ni(001). However, comparison of the local densities of the electronic states (LDOS) for the unreconstructed and reconstructed structures, does not exhibit any tractable modification upon reconstruction.

Thus, despite a volume of effort, the factors responsible for C induced reconstruction of Ni(001) remain to date unclear. These studies also emphasize the need for a more detailed description of the electronic structure, the character of chemical bonding and the energetics of the system. Since the reconstruction is found to commence at a specific C coverage ($\theta \approx 0.33$ ML), it is also important to compare and contrast the electronic structures of C _{θ} /Ni(001) with $\theta < 0.33$ ML and $\theta > 0.33$ ML.

In this paper, we present the results of our calculations of the geometric and electronic structure of C/Ni(001) performed for coverages of 0.25 ML [$p(2 \times 2)$] and 0.5 ML [$c(2 \times 2)$] within the density functional theory with the generalized gradient approximation for the exchange-correlation potential. Applying a structural optimization procedure within the PWPP method, we reproduce the reconstruction for C_{0.5}/Ni(001) and provide the energetics and path of transition from the $c(2 \times 2)$ to the $p4g$ geometry. The valence charge densities and local valence charges are then calculated using a more accurate technique for the purpose which is based on the full potential linearized augmented plane wave (FLAPW) method. A comparison of the modifications in the characteristics of the surface as the coverage changes from 0.25 ML to 0.5 ML, provides a consistent description of the mechanism responsible for the reconstruction.

II. COMPUTATIONAL DETAILS

All calculations presented in this paper have been performed within the density functional theory with the gener-

alized gradient approximation (GGA) for the exchange-correlation functional.¹⁵ The Ni(001) surface was modeled by a tetragonal supercell consisting of a 7 layer Ni slab and 11 Å of vacuum. For both 0.25 ML and 0.5 ML carbon coverages we have used a two dimensional (2×2) unit cell. The supercell also contains two C atoms (one atom on each side of the Ni slab) for the 0.25 ML coverage, and four C atoms (two atoms on each side of the slab) for the 0.5 ML coverage. Thus, the supercells consist of 30 and 32 atoms, for 0.25 ML and 0.5 ML coverages, respectively.

Surface geometry and energetics have initially been calculated using the PWPP method¹⁶ with ultrasoft pseudopotentials¹⁷ for C and Ni. We set cutoff energies for the plane-wave expansion of 300 eV for both clean and C-covered surfaces and used a $5 \times 5 \times 1$ Monkhorst-Pack k -point mesh for sampling the Brillouin zone.¹⁸ The structures were optimized until the forces acting on each atom converged better than 0.01 eV/Å.

These optimized structures were then used as input for a more detailed analysis of the electronic structure, which includes self-consistent calculations of the valence charge density and local charges of the systems, using the full potential linearized augmented plane wave (FLAPW) method¹⁹ as embodied in the computational code Wien2k²⁰ which further refined the geometries after a few ionic iterations. To be consistent, we have used the same supercells and k -point mesh in the Brillouin zone for the FLAPW and PWPP calculations. Note that in the FLAPW method, the local charges are calculated through integration over muffin-tin (MT) spheres of radius R_{MT} centered at each atom. To analyze the effect of the adsorbate on these specific quantities the set of R_{MT} should be chosen to be the same for all structures under consideration. Ideally, R_{MT} should be as large as possible without causing the MT spheres to overlap. For the inner atoms of the Ni slab, including those in the second layer, a choice of $R_{MT} = 1.19$ Å is optimal. However, more compatibility with the shorter C-Ni bond lengths is provided with $R_{MT} = 1.005$ Å for Ni1 and $R_{MT} = 0.773$ Å for C. To keep plane-wave cutoff at a reasonably high value ($RK_{max} = 7$) with the reduced R_{MT} 's for the surface atoms, we used basis sets of about 5500 LAPW's including 256 local orbitals for the surface with 0.25 ML C and the reconstructed surface with 0.5 ML coverage, and 2800 LAPW's including 128 local orbitals, for the unreconstructed surface with 0.5 ML coverage.

III. RESULTS AND DISCUSSION

A. Carbon induced structural modification of Ni(001)

1. The effects of 0.25 ML C on an Ni(001) geometric structure

To our knowledge, the case of 0.25 ML C on Ni(001) has not been studied so far using first principles calculations based on density functional theory. We have carried out such calculations of the geometric structure of the system using a structural optimization procedure that minimizes the forces applied to the atoms. We find our results to be in a good agreement with experimental observations. Namely, computational structural optimization does not lead to the $p4g$ re-

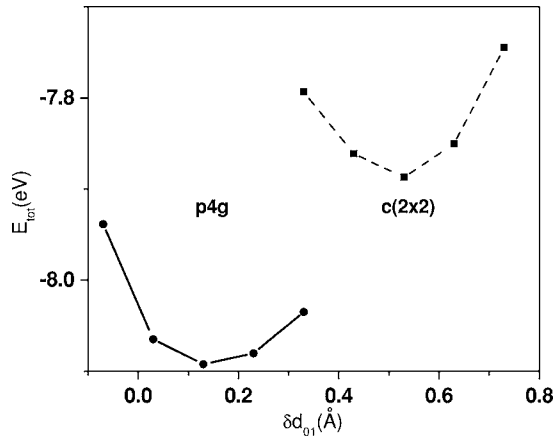


FIG. 2. Dependence of the total energy versus the C-Ni1 separation calculated for $C_{0.5}/Ni(001)$ in $c(2 \times 2)$ and $p4g$ geometries. Zero energy corresponds to C desorption.

construction in this system and results in a stable $p(2 \times 2)$ geometry. Even when we shift initially the Ni1 atoms along the $p4g$ reconstruction path, they revert to the $p(2 \times 2)$ geometry during the optimization. We also find that the presence of C causes radial outward displacement $\Delta r = 0.07 \text{ \AA}$ of the Ni1 atoms from their equilibrium positions on the clean surface. This result is in qualitative agreement with experimental observations which report such outward displacements ranging from $0.02 \pm 0.03 \text{ \AA}$ (for 0.15 ML coverage)⁴ to $0.15 \pm 0.15 \text{ \AA}$ (for about 0.2 ML coverage).³ Our calculated equilibrium C-Ni1 separation $d_{01} = 0.24 \text{ \AA}$ is also in reasonable agreement with that ($0.21 \pm 0.07 \text{ \AA}$) obtained for $C_{0.15}/Ni(001)$ from PhD measurements.⁴

2. The Effects of 0.5 ML C on Ni(001) geometric structure

We start our calculation of $C_{0.5}/Ni(001)$ with the perfect $c(2 \times 2)$ structure, and calculate the total energy (E_{tot}) of the system as a function of d_{01} . At each step we fix the C position and let the rest of the atoms relax (move in any direction). The result of these calculations is shown in the curve on the right side of Fig. 2. No reconstruction occurs during structural optimization and a E_{tot} minimum is found at $d_{01} = 0.53 \text{ \AA}$. Next, we repeat the procedure, but starting with the surface Ni atoms (Ni1) initially in the $p4g$ reconstructed geometry with lateral displacements Δxy taken from experimental measurements.⁴ Since the nickel atoms are free to relax as the C atoms are lowered, the system finds the stable position of Ni1. We find that although Ni1 positions change during optimization depending on d_{01} , the system is kept in the $p4g$ structure.

Since Ni is a ferromagnetic metal, we perform these calculations for both nonmagnetic and spin-polarized ferromagnetic cases. The values of d_{01} and the lateral Ni1 displacement Δxy obtained for the equilibrium (minimum E_{tot}) structures from these two calculations are listed in Table I together with those measured in the experiments. As seen from the table, the spin polarization effect on the geometric structure is negligible and both calculated structures are in very good agreement with the experimental observations. To

TABLE I. Comparison of structural parameters of $C_{0.5}-p4g/Ni(001)$ calculated in this work with those obtained from experiments (Refs. 4 and 5). NM and FM denote nonmagnetic and ferromagnetic calculations, respectively.

	d_{01} (Å)	Δxy (Å)
NM	0.13	0.51
FM	0.14	0.51
Exper.	0.1-0.12	0.41-0.55

understand why the magnetic effect on the geometric structure is so small, we calculate local Ni spins in the system by integrating spin density over the spheres of 1.2 \AA radius centered at different Ni atoms. We find that while the spin on the Ni atoms located at the center of the slab equals $0.69 \mu_B$, it is reduced to $0.39 \mu_B$ on Ni2 neighboring carbon and is diminished to $0.02 \mu_B$ on Ni1. This result indicates that strong covalent C-Ni bonding suppresses spin polarization on the Ni atoms surrounding adsorbed C and makes it possible to neglect the magnetic effects on the $C/Ni(001)$ surface geometric structure. We thus perform all of the following calculations for nonmagnetic systems.

The $E_{tot}(d_{01})$ dependence calculated for the nonmagnetic $p4g$ structure is plotted on the left side of Fig. 2. One can see that the E_{tot} minimum for the $p4g$ structure is about 0.8 eV lower than that for the $c(2 \times 2)$ one. At first sight, both dependencies shown in Fig. 2 suggest that the system has two energy minima: the local one for the $c(2 \times 2)$ structure and the global one for the reconstructed $p4g$ structure and there is an energy barrier between them. However, our further consideration shows that this is a wrong conclusion. C adsorbed in the ideal $c(2 \times 2)$ structure cannot induce forces acting on Ni atoms along any direction, which breaks the $c(2 \times 2)$ symmetry. Regular optimization procedures applying the quasi-Newton or conjugate gradient methods are thus not able to lead such a system to reconstruction. In reality, even if the system appears to be in the $c(2 \times 2)$ structure, atomic vibrations naturally break the symmetry that can cause the forces leading to the reconstruction.

To place these speculations on firmer ground, we perform another calculation starting with a system slightly deviated from the (2×2) symmetry. Namely we start with the quasi-equilibrium $c(2 \times 2)$ structure obtained above, but with Ni1 atoms slightly shifted along the reconstruction path ($\Delta xy = 0.01 \text{ \AA}$) and let all atoms relax. We find that the structural optimization leads $C_{0.5}/Ni(001)$ to the equilibrium $p4g$ structure with parameters d_{01} and Δxy practically the same as obtained in the simulation described above. The system thus undergoes a $c(2 \times 2)-p4g$ transformation without any energy barrier that is in agreement with the conclusion made in Ref. 12. This finding is illustrated in Fig. 3. Since in the course of the reconstruction Δxy , the lateral Ni1 displacements, and C-Ni1 height d_{01} change simultaneously, the reconstruction path is well-characterized by the dependence $d_{01}(\Delta xy)$ plotted in Fig. 3. To illustrate energetics of the reconstruction, we also plot the variation E_{tot} versus Δxy (E_{tot} of the starting configuration is a reference point for ΔE_{tot}). As seen from the

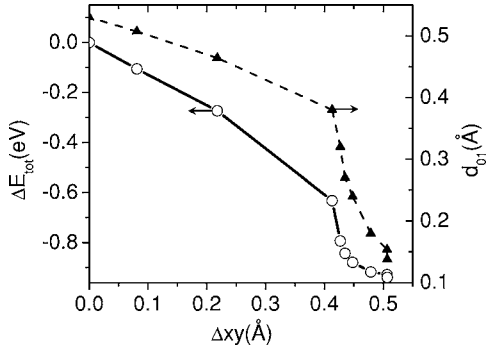


FIG. 3. The reconstruction path and energetics calculated for $C_{0.5}/Ni(001)$: the C-Ni1 height (dashed line) and a variation of the total energy of the system (solid line) are plotted versus lateral displacement of Ni1 atoms happened during the reconstruction.

figure, there is no activation barrier for the reconstruction and there is a close correlation between d_{01} and E_{tot} . Both characteristics change smoothly and gradually as long as $\Delta xy \leq 0.4$ Å. As Δxy exceeds this value, both d_{01} and E_{tot} decrease sharply. The rationale for such behavior will be discussed in the next subsection together with results of the calculations of the valence charge density.

B. Electronic Structure of C/Ni(001)

Having shown that the structural behavior of C/Ni(001) obtained from calculations based on the PWPP method completely reproduces experimental observations, we now move on to reveal the factors controlling the clock reconstruction. To this end, we analyze the relationship between the geometric and electronic structures of the system using the results that we obtain from application of the FLAPW method which provides a higher level of accuracy and detail, as compared to the PWPP method. We calculate the electronic structure for the two stable structures seen in experiments: $p(2 \times 2)C_{0.25}/Ni(001)$ and $p4gC_{0.5}/Ni(001)$, as well as, for two hypothetical $c(2 \times 2)C_{0.5}/Ni(001)$ structures: one with quasi-stable geometry ($d_{01} = 0.53$ Å) and another with a reduced C-Ni1 separation ($d_{01} = 0.38$ Å). Figures 4–7 show the valence charge densities calculated for these structures and plotted along a (010) plane, which crosses the C atom. We find strong covalent C-Ni1 bonds to be formed in all four structures. These bonds are seen in the figures as “bridges” of electronic density between the C and Ni1 atoms. Additionally, the $p(2 \times 2)C_{0.25}/Ni(001)$ and $p4gC_{0.5}/Ni(001)$ structures display distinct covalent “bridges” between the C and Ni2 atoms—a feature missing in both $c(2 \times 2)C_{0.5}/Ni(001)$ structures. This extra covalent bond naturally increases stability of the system by reducing its total energy as can be seen from the correlation between E_{tot} and d_{01} as shown in Fig. 3. As d_{01} decreases, the C-Ni2 bonds shorten, enhancing the C-Ni2 covalent bonding and reducing the total energy. The sharp reduction of E_{tot} at lower values of d_{01} (Fig. 3) reflects the fact that the covalent bonding involves the localized $3d$ -states of Ni2.

The question that emerges is: why are C-Ni2 bonds not formed in $c(2 \times 2)C_{0.5}/Ni(001)$? For an answer we turn to

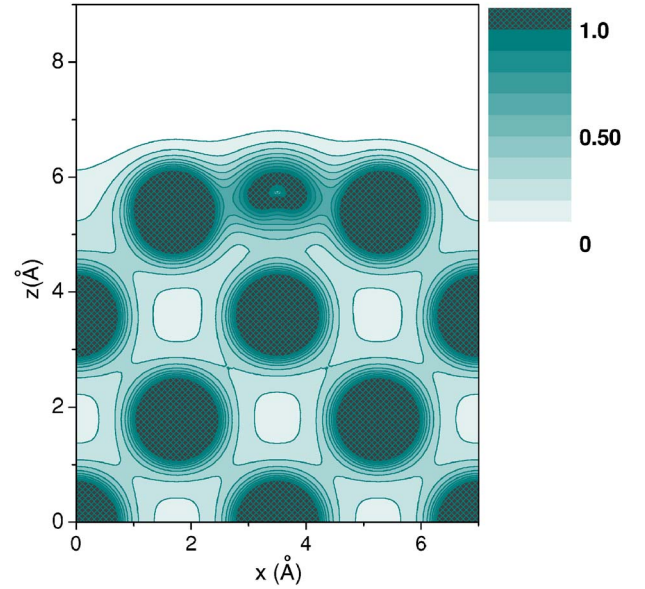


FIG. 4. (Color online) The valence charge density calculated for $p(2 \times 2)C_{0.25}/Ni(001)$ and plotted along a (010) plane, which crosses the center of C atom. The black solid line in the upper panel of Fig. 1 marks a projection of this plane onto the surface.

the measures of the C-Ni2 bond lengths (l_{C-Ni2}) for the four C/Ni(001) structures, as determined by our calculations. These are summarized in Table II together with those for the C-Ni1 bond lengths (l_{C-Ni1}). Clearly, the bond length for C-Ni2 is smaller and closer to that for C-Ni1 for the two stable structures, as compared to those for the unstable $c(2 \times 2)$ structures. Interestingly, as l_{C-Ni2} reduces from 2.33 Å to 2.18 Å in $c(2 \times 2)C_{0.5}/Ni(001)$, the total energy of the system increases (see Fig. 2). Actually this counterintuitive

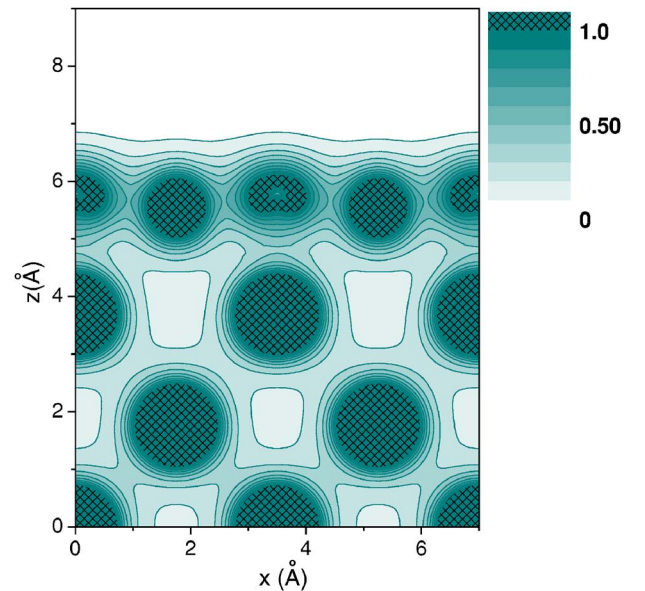


FIG. 5. (Color online) The same as in Fig. 4, but for $p4gC_{0.5}/Ni(001)$. Note that the (010) plane, along which the charge density is plotted, does not cross the centers of Ni1 atoms in this reconstructed structure (see the lower panel of Fig. 1).

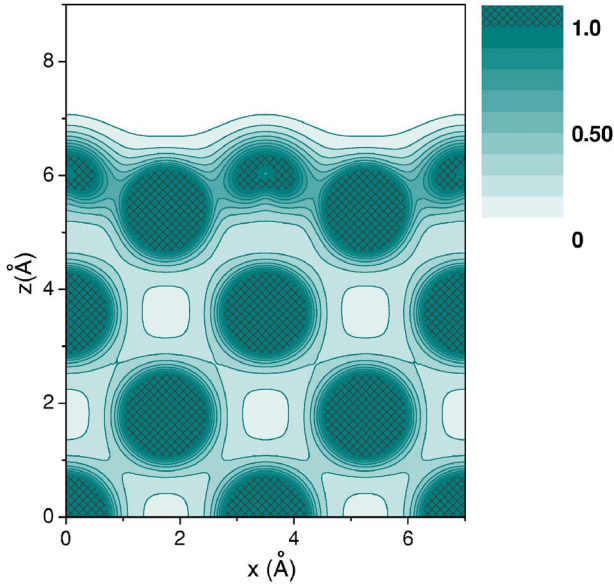


FIG. 6. (Color online) The same as in Fig. 4, but for $c(2 \times 2)C_{0.5}/Ni(001)$ with $d_{01} = 0.53 \text{ \AA}$.

behavior of the increase in the total energy of the system with decrease in the C-Ni2 bond length for the $c(2 \times 2)$ structure provides a clue as to why this surface reconstructs once we take into consideration the local charges on the C atoms.

The local charges $Q_{MT}(C)$, calculated by integrating the valence charge density over the C muffin-tin sphere with $R_{MT} = 0.773 \text{ \AA}$, are listed in Table III. We find that when l_{C-Ni2} in $c(2 \times 2)C_{0.5}/Ni(001)$ is reduced by 0.25 \AA (as d_{01} changes from 0.53 \AA to 0.38 \AA), $Q_{MT}(C)$ increases substantially. As seen from Table II this decrease in l_{C-Ni2} is accompanied by a reduction of l_{C-Ni1} . Apparently, as l_{C-Ni1} becomes shorter, neighboring Ni1 atoms compress the electronic

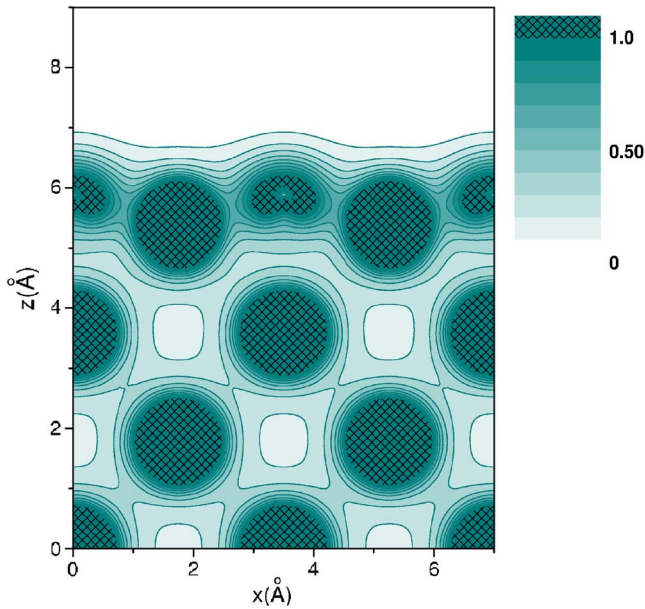


FIG. 7. (Color online) The same as in Fig. 4, but for $c(2 \times 2)C_{0.5}/Ni(001)$ with $d_{01} = 0.38 \text{ \AA}$.

TABLE II. C-Ni bond lengths calculated for the considered C/Ni(001) structures.

	$l_{C-Ni1}(\text{\AA})$	$l_{C-Ni2}(\text{\AA})$
$p4g-C_{0.5}$	1.83	1.99
$p(2 \times 2)-C_{0.25}$	1.83	2.04
$c(2 \times 2)-C_{0.5}, d_{01}=0.38$	1.79	2.18
$c(2 \times 2)-C_{0.5}, d_{01}=0.53$	1.83	2.33

charge density on carbon atoms, which in turn enhances the electron-electron repulsion on the C atoms contributing to the increase in the total energy mentioned above. The reduction of l_{C-Ni1} is understandable since in $c(2 \times 2)C_{0.5}/Ni(001)$ there is no room for an outward displacement of Ni1 atoms. As the clock reconstruction takes place, l_{C-Ni1} increases and $Q_{MT}(C)$ decreases dramatically. It should be noted that $Q_{MT}(C)$ in the stable $p(2 \times 2)C_{0.25}/Ni(001)$ structure is also significantly smaller than that in the unstable $c(2 \times 2)$ structures. However, the C-Ni1 bond length is not the only factor controlling $Q_{MT}(C)$. When the C-Ni2 covalent bond is formed some portion of the valence electron density is transferred to the C-Ni2 covalent “bridge.” This is seen from the comparison of $Q_{MT}(C)$ in Table III for $p(2 \times 2)C_{0.25}/Ni(001)$, $p4gC_{0.5}/Ni(001)$, and $c(2 \times 2)C_{0.5}/Ni(001)$ with $d_{01} = 0.53 \text{ \AA}$. All three structures have $l_{C-Ni1} = 1.83 \text{ \AA}$ (see Table II), but different $Q_{MT}(C)$. The C-Ni2 covalent bond is not formed in $c(2 \times 2)C_{0.5}/Ni(001)$, and $Q_{MT}(C)$ is the largest in this system. On the other hand, $p4gC_{0.5}/Ni(001)$ has the strongest C-Ni2 covalent bond and the lowest value of $Q_{MT}(C)$. We thus find two factors that make the $c(2 \times 2)-p4g$ reconstruction favorable in $C_{0.5}/Ni(001)$: formation of the C-Ni2 covalent bond that reduces the energy of the system and reduction of $Q_{MT}(C)$ that prevents a strong electron-electron repulsion on carbon.

As an aside, we comment here on the possible effect of dipolar interaction on the reconstruction mechanism.⁹ Since the work functions Φ of the systems reflect changes in the dipole moments, we have included in Table III their calculated values for the structures of interest here. While there is some correlation between Φ and the C-Ni1 separation, the in-plane displacements of the Ni1 atoms do not impact Φ in a consistent manner, thereby suggesting that dipole-dipole interaction does not control the reconstruction of C/Ni(001).

In summary, we have performed first principles calculations of the geometric and electronic structures of C/Ni(001)

TABLE III. C local charges and work functions calculated for the C/Ni(001) structures.

	$Q_{MT}(C)$	$\Phi(\text{eV})$
$c(2 \times 2)-C_{0.5}, d_{01}=0.53 \text{ \AA}$	4.58	5.67
$c(2 \times 2)-C_{0.5}, d_{01}=0.38 \text{ \AA}$	4.67	5.55
$p4g-C_{0.5}, d_{01}=0.13 \text{ \AA}$	4.30	5.39
$p(2 \times 2)-C_{0.25}, d_{01}=0.24 \text{ \AA}$	4.41	5.35

with the C coverages of 0.25 and 0.5 ML. The structural behavior of the system obtained from the calculations is in a good agreement with experimental observations. No energy barrier is found on the reconstruction path. We find that formation of the C-Ni2 covalent bonds is crucial for the stability of C/Ni(001). These bonds are present in the stable $p(2 \times 2)C_{0.25}/Ni(001)$ and $p4gC_{0.5}/Ni(001)$ structures and absent in unstable $c(2 \times 2)C_{0.5}/Ni(001)$. Apart from formation C-Ni2 covalent bond, the $c(2 \times 2)$ - $p4g$ reconstruction in $C_{0.5}/Ni(001)$ is accompanied by a dramatic reduction of the

local electronic charge on adsorbed carbon that decreases the electron-electron repulsion on C site and lowers the total energy of the system.

ACKNOWLEDGMENTS

A grant from NCSA, Urbana, IL was beneficial in providing computational resources. We acknowledge financial support from the NSF, under Grant No. CHE-0205064.

-
- ¹I. S. Stolbov, F. Mehmood, T. S. Rahman, M. Alatalo, I. Makkonen, and P. Salo, *Phys. Rev. B* **70**, 155410 (2004).
²J. N. Onuferko, D. P. Woodruff, and B. W. Holland, *Surf. Sci.* **87**, 357 (1979).
³C. Klink, L. Olesen, F. Besenbacher, I. Stensgaard, E. Laegsgaard, and N. D. Lang, *Phys. Rev. Lett.* **71**, 4350 (1993).
⁴R. Terborg, J. T. Hoefl, M. Polcik, R. Lindsay, O. Schaff, A. M. Bradshaw, R. L. Toomes, N. A. Booth, D. P. Woodruff, E. Rotenberg, and J. Denlinger, *Surf. Sci.* **446**, 301 (2000).
⁵Y. Gauthier, R. Baudoing-Savois, K. Heinz, and H. Landskron, *Surf. Sci.* **251-252**, 493 (1991).
⁶T. S. Rahman and H. Ibach, *Phys. Rev. Lett.* **54**, 1933 (1985).
⁷T. S. Rahman, *Phys. Rev. B* **35**, 9494 (1987).
⁸C. Q. Sun and P. Hing, *Surf. Rev. Lett.* **6**, 109 (1999).
⁹C. Q. Sun, *Surf. Rev. Lett.* **7**, 347 (2000).
¹⁰J. E. Müller, M. Wuttig, and H. Ibach, *Phys. Rev. Lett.* **56**, 1583 (1986).
¹¹D. Sander, U. Linke, and H. Ibach, *Surf. Sci.* **272**, 318 (1992).
¹²D. Alfe, S. de Gironcoli, and S. Baroni, *Surf. Sci.* **437**, 18 (1999).
¹³S. Hong, A. Kara, T. S. Rahman, R. Heid, and K. P. Bohnen, *Phys. Rev. B* **69**, 195403 (2004).
¹⁴J. E. Kirsch and S. Harris, *Surf. Sci.* **522**, 125 (2003).
¹⁵J. P. Perdew and Y. Wang, *Phys. Rev. B* **45**, 13244 (1992).
¹⁶M. C. Payne, M. P. Teter, D. C. Allan, T. A. Arias, and J. D. Joannopoulos, *Rev. Mod. Phys.* **64**, 1045 (1992).
¹⁷D. Vanderbilt, *Phys. Rev. B* **41**, R7892 (1990).
¹⁸H. J. Monkhorst and J. D. Pack, *Phys. Rev. B* **13**, 5188 (1976).
¹⁹M. Weinert, E. Wimmer, and A. J. Freeman, *Phys. Rev. B* **26**, 4571 (1982); D. Singh, *Planewaves, Pseudopotentials and the LAPW Method*, (Kluwer Academic Publishing, Dordrecht (1994).
²⁰P. Blaha, K. Schwarz, G. K. H. Madsen, D. Kvasnicka, and J. Luitz, *WIEN2k, An Augmented Plane Wave and Local Orbitals Program for Calculating Crystal Properties* (Karlheinz Schwarz, Technical Universität Wien, Austria) 2001.